Chemistry–A European Journal

Research Article
doi.org/10.1002/chem.202404200

Chemistry Europe
European Chemical Societies Publishing

www.chemeurj.org

Photocatalyzed Dehydration of 1-Aryl-1,2-Ethanediols to Methyl Ketones Driven by Eosin Y Fragmentation Products

Elina K. Taskinen,[a] Daniel Kolb,[a] Martin Morgenstern,[a] and Burkhard König*[a]

Herein, we report a mild photocatalytic redox-neutral dehydration of aryl-1,2-ethanediols forming the respective methyl ketones. In the proposed mechanistic cycle an initial hydrogen atom abstraction (HAT) is followed by a 1,2-spin center shift (SCS) as key steps. Interestingly, Eosin Y was found to act as a pre-catalyst dissociating into a catalytically active mixture under irradiation. To the best of our knowledge, this exemplifies the first synthetic utilization of Eosin Y degradation products. As a result, our reaction can be realized with a single organic photocatalyst and releases water as a sole by-product.

Introduction

1,2-Diols and vicinal polyols are widely present in Nature, playing vital roles in the structure and function of life-enabling architectures.[1] For plants and bacteria, carbohydrates represent the main constituent in their cell walls. For mammals, carbohydrates form the backbone for genetic information storage (deoxyribose in DNA) and are a major energy source.[2] Furthermore, glycosylation, the addition of glycans to cell surfaces, has been identified as an efficient means for cell-to-cell signalling and pathogen recognition in the recent years.[3] In society, naturally occurring polyols have found various uses as food additives (Xylitol), dyes (anthocyanins), and cosmetics (glycerine).[4] In chemistry, polyols have served as important building blocks for the chiral pool and provided inspiration for method development for decades.[5] As a result, the reactivity of alcohols has been carefully studied and further utilized in the synthesis of polymers or polyhydroxylated natural products.[6,7]

Recently, the well-established two-electron transformations of alcohols have been enriched further by photochemistry, which provides a mild and easy access to one-electron reaction pathways.[8] The reactivity of oxygen-centered radicals, generated from ligand-to-metal charge transfer (LMCT) or proton coupled electron transfer (PCET) strategies have unlocked several intriguing transformations ranging from hydrogen atom transfer (HAT) to selective C–C bond cleavage.[8a,b,f] For instance, when subjecting diol **I** to cerium LMCT catalysis, the initial formation of an oxygen-centered radical is swiftly followed by a β-scission forming the corresponding aldehyde products **II** and **III** (Scheme 1a).[9] In addition to the alkoxy radical generation, the proximity of a heteroatom also lowers the dissociation energy of the neighbouring C–H bonds,[10] thus providing means for highly selective α-O activation strategies (Scheme 1b–1d). Although in many cases the transient carbon-centered radical (such as **VII**) is trapped by radical acceptors, the same intermediate has also been utilized in C–O-epimerizations as elegantly demonstrated by the groups of MacMillan, Phipps and Wendlant (Scheme 1b, compounds **V** and **VI**).[11] Upon further tuning the reaction conditions, the α-oxygen radicals **VII** and **XI** can be directed towards another reaction pathway. As first defined by Wessig and Muehlin in their review article, the classical 1,2-spin center shift (SCS) process can be described as "a 1,2- radical shift accompanied by the elimination of an adjacent leaving group or its corresponding acid".[12] Inside living cells, the SCS sequence works as a key step

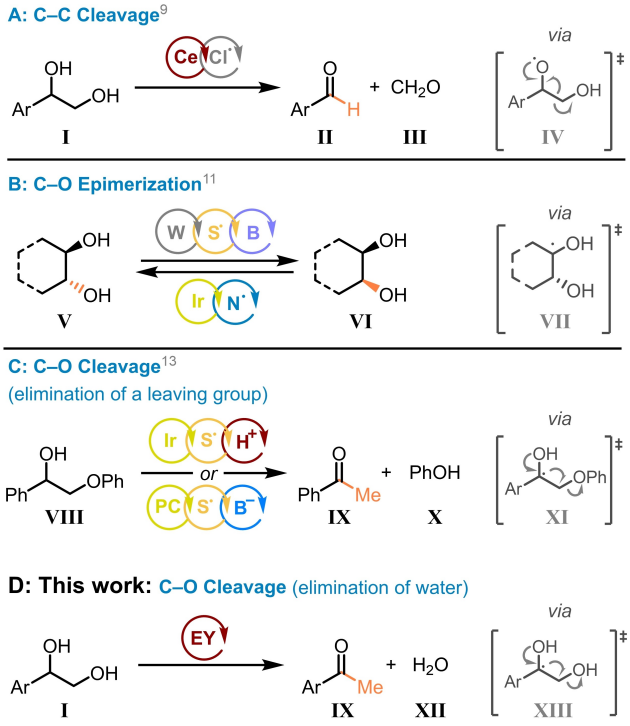

Scheme 1. Previous reported photocatalytic reactions of vicinal diols (a–c)[9,11,13] and the redox-neutral photocatalytic dehydration (this work, d).

[a] E. K. Taskinen, D. Kolb, M. Morgenstern, B. König
Department of Chemistry and Pharmacy, University of Regensburg, Universitätstr. 31, 93053 Regensburg, Germany
E-mail: burkhard.koenig@ur.de

Supporting information for this article is available on the WWW under https://doi.org/10.1002/chem.202404200

in the biosynthesis and repair of DNA, yet due to the effortless engagement of multiple atoms, this process has also found its use in organic chemistry.[12] For synthetic purposes, the SCS has been used in intermolecular and intramolecular reactions to achieve a wide array of transformations ranging from pyridine alkylations to degradation of lignin model compounds.[13] Towards the latter goal, the groups of König and Nocera have harnessed a dual-catalytic system comprising of a photocatalyst and HAT catalyst for the redox-neutral phenolate elimination (Scheme 1c).[14] Despite the success of this dual catalytic strategy on lignin-like compounds, no reaction could be observed with a free hydroxy group as the leaving group. As summarized by Houk and Wang in their recent review, the general limitation still suppressing the broader applicability of the SCS is its requirement for a good leaving group and/or for additives to assist the elimination.[13a] As converting the β-functionality to a good leaving group adds to the number of synthetic steps and increases the waste generated, the use of strong acids or bases severely limits the functional group tolerance. To address these limitations, we herein report a redox-neutral photocatalytic HAT/SCS sequence for the mild dehydration of aryl-1,2-ethanediols **I** to methyl ketones (Scheme 1d). Our reaction runs with a single organic photocatalyst thus providing a significant simplification to the previously reported catalytic systems. Moreover, substrate preactivation together with acidic or basic additives can be avoided. As a result, water is released as the sole by-product of our reaction.

Results and Discussion

Reaction Optimization

We commenced our efforts towards the development of a mild dehydration protocol by choosing the commercially available 1-phenyl-1,2-ethanediol (**1a**) as a starting material (Table 1). Upon screening various HAT catalysts, we were pleased to observe that Eosin Y gave an excellent conversion of the starting material into the product within one hour (Table S1). With further optimization, the loading of Eosin Y could be reduced to 2 mol% while obtaining the product in 91% yield (Entry 1). Intriguingly, the structurally related Fluorescein and product-resembling benzophenone were unable to catalyse the desired transformation (Entries 2 and 3). Bismuth and iron chloride, known to generate chlorine radicals *via* LMCT mechanism,[15] also furnished the product albeit in lowered yields (32% and 11% yield, respectively, Entries 4 and 5). Moving on to solvents, acetonitrile turned out to be the best option, although ethyl acetate also gave good yields yet the reaction was proceeding slightly slower (Entry 6). Unexpectedly, the irradiation with 385 nm LEDs gave the highest yield, whereas 520 nm or 420 nm irradiation resulted in trace amounts of product (Entry 7).

Finally, control experiments proved the necessity of an inert atmosphere, light and photocatalyst for the transformation (Entries 8 and 9).

Table 1. Screening of reaction conditions.

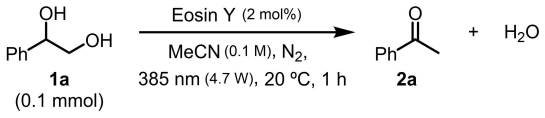

1a (0.1 mmol) **2a**

Entry	Deviation from optimal	Yield (%)[a]
1	None	91
2	Fluorescein	0
3	Benzophenone	0
4[b]	$BiCl_3$ (20 mol%)	32
5[c]	$FeCl_3$ (20 mol%)	11
6[d]	EtOAc instead of MeCN	73
7	420 nm or 520 nm LEDs	*traces*
	Control Experiments	
8	Under Air	*traces*
9	No light or Photocatalyst	0

[a] Yields calibrated GC-FID yields. [b] $BiCl_3$ (20 mol%) + TBACl (40 mol%). [c] $FeCl_3$ (20 mol%) + TBACl (20 mol%). [d] Reaction time 3 h. TBACl = tetra-*n*-butylammonium chloride.

Substrate Scope

Having established the optimal reaction conditions, we moved on to study the scope of the transformation. Some trends across the reaction scope were identified (Scheme 2). With respect to the steric effects, a methyl substituent on the *para*- and *meta*-positions gave essentially identical yields (71% and 70%), whereas shifting the methyl group to the *ortho*-position decreased the yield to 21% (compound **2b** + **2c** vs. **2d**). These results suggest some degree of sensitivity towards steric hindrance near the reaction center. Further away on the ring, though, a smooth conversion to the product could be achieved even with a *tert*-butyl group in place (compound **2e**).

With respect to the electronic effects, a clear preference was observed for electron-poor groups placed in the *para*-position and electron donating groups located in the *meta*-position (*vide infra*). For example, the *para*-fluorinated diol furnished the corresponding acetophenone **2f** in a 72% yield whereas the *meta*-fluorinated diol reacted to the product in a mere 32% yield (**2g**).

In addition to fluorine, trifluoromethyl and chlorine *para*-substituents were also well tolerated, both giving the desired products with over 70% yields (compounds **2h** and **2i**). In contrast, a methoxy group in a *para*-position led to 15% yield of product **2j** but a methoxy group as the *meta*-substituent gave the acetophenone derivative **2k** in an excellent yield (91%). Furthermore, a highly electron-rich and acid-labile TBS group could be used to protect the phenolic hydroxy group in the *meta*-position, thus forming the corresponding OH-protected acetophenone **2l** in a 68% yield. A MOM-protected phenol, in turn, gave the product **2m** in 11% yield. Mechanistically speaking, the observed electronic preference seems to support the HAT as a mechanism for the initial radical

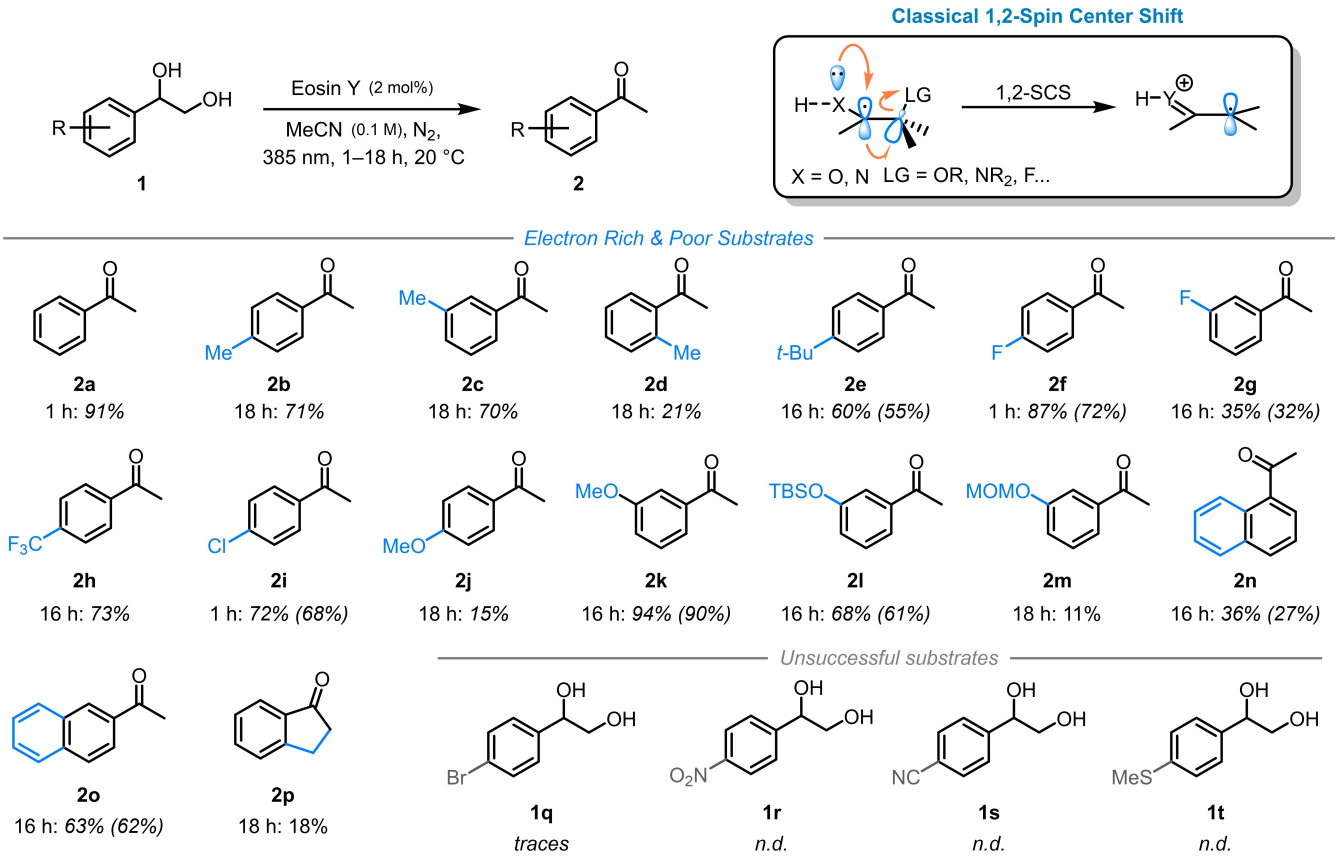

Scheme 2. Scope for the photocatalytic dehydration of diols. Yields reported as calibrated GC-FID yields, isolated yields in parenthesis.

generation as the alternative aryl oxidation-deprotonation pathway would operate better on electron-rich aromatic systems.[16]

Moving on to the naphthyl system, the sterically hindered 1-napthyl diol reacted to the corresponding acetophenone product **2n** more sluggishly than its 2-napthyl counterpart **2o**. Lastly, the importance of free rotation and antiperiplanar relationship between the leaving group and the benzylic radical were showcased by the thwarting of the reaction with substrate **2p** where the leaving group is located on a secondary carbon (see also SI). Regarding limitations, the bromine-containing substrate **1q** decomposed under the reaction conditions, whereas cyano-, nitro- and sulfur-containing groups completely prevented the reaction progress (substrates **1r**–**1t**).

Mechanistic Studies

To gain a deeper understanding of our reaction, a set of mechanistic experiments was carried out. Our initial hypothesis was that the neutral Eosin Y, which has been well-established as a HAT catalyst, would be the catalytically active species in our reaction.[17] However, we were puzzled by the identification of 385 nm LEDs as optimal irradiation source and the lack of reactivity with 420 nm and 520 nm irradiation (Table 1 and Table S4). Therefore, we started out by tracking down the light-absorbing species in our reaction mixture. When dissolved into acetonitrile, the main absorption band of the Eosin Y was found around 540 nm (Figure 1b). As this absorption band has been assigned to the monoanionic Eosin Y, our observation further demonstrates this photocatalyst's dynamic, solvent-dependent acid-base equilibrium.[17b,c] Although protonation of Eosin Y with Brønsted acids has been reported to enhance the HAT-activity of the catalyst, in our system, the addition of acetic acid, hydrochloric acid or sulfuric acid did not enable the conversion *trans*-cyclohexane-1,2-diol to cyclohexanone.[17d] This result further implied that our reaction might not proceed *via* excitation of neutral Eosin Y. Upon a careful inspection, an additional absorption feature can be observed around 380 nm.[18] This band was unambiguously identified to stem from Eosin Y (dark orange line), whereas the diol **1a** did not show any absorbance above 300 nm (grey dotted line). However, the addition of **1a** to a solution of Eosin Y resulted in small changes in the absorption spectrum on both sides of the utilized irradiation wavelength, thus indicating a possible hydrogen bonding and/or π-π-stacking interactions between these species.

To better characterize the observed colour change of the reaction mixture from bright pink to pale yellow under irradiation (Figure 1a), an *ex-situ* UV-vis monitoring of the reaction was carried out. Irradiation with a 385 nm LED resulted in a smooth decrease in the Eosin Y main absorption band at 520 nm, followed by the rise of a broad absorption band in the

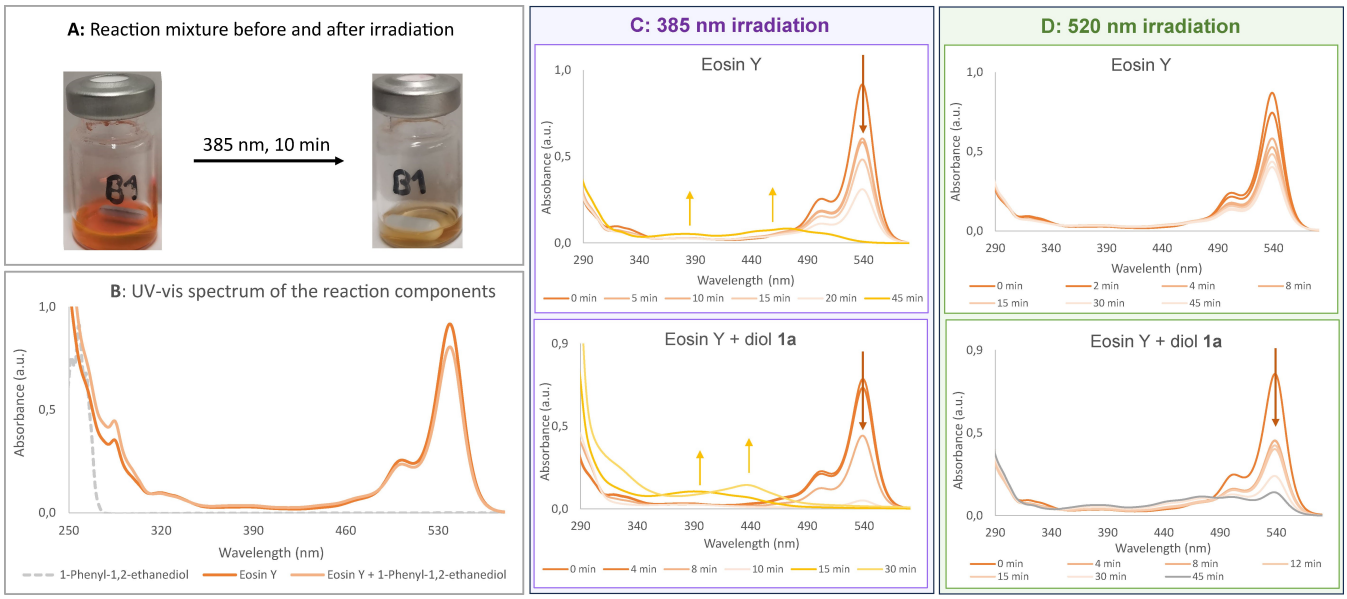

Figure 1. The observed colour change of the reaction mixture (a), UV-vis spectrum of the reaction components separately and together in MeCN (b), spectral changes observed in *ex situ* UV-vis measurements upon irradiating with 385 nm LEDs (c) and 520 nm LEDs (d).

blue-light region (Figure 1c). Noteworthily, the diol **1a** had a significant impact on the rate of the spectral changes: a solution containing only Eosin Y retained its green-light absorption band for almost 45 minutes, whereas in the presence of the diol, this band disappeared after 10 minutes of irradiation. Although faster, these spectral changes are in good agreement with those observed by the group of Janssen during their study on the Eosin Y photodegradation under green laser irradiation.[19] Under a green-light LED, however, our spectral changes were significantly slower and without the diol **1a** no new absorption features could be observed (Figure 1d). These differences observed with different irradiation sources might stem either from the higher energy and higher light intensity of the 385 nm LEDs and 520 nm laser as compared to 520 nm LEDs or, alternatively, hint towards excitation of an electron to a higher laying orbital when using a lower wavelength irradiation (anti-Kasha behaviour).[20] Further support to the hypothesis of Eosin Y photolysis was obtained from HPLC-MS analysis of the reaction mixture which revealed the emergence of numerous compounds after a 10 minute irradiation period. Based on HRMS, most of these molecules could be categorized into a) debromination, b) dehydration, and c) radical adducts of Eosin Y (Scheme 3a and Figure S10). In this context, it is also worth mentioning that the control experiment of stirring Eosin Y at 60 °C in the dark did not result in any degradation even after prolonged periods of time, thus confirming the photochemical nature of this process.

We then turned our attention to the product-forming events. The kinetic profile of the reaction was measured and was found to display a sigmoidal curve (Scheme 3b). Furthermore, three different stages could be separated from this curve: the reaction starts with an induction period (stage I, 0–10 min), followed by rapid consumption of the substrate (stage II, 10–15 min) and ending with a prolonged period of continuous product formation (stage III, 15–60 min). Strikingly, when comparing the reaction kinetics with the UV-vis studies on Eosin Y degradation discussed above, the time frame for the induction period and photodissociation of the catalyst seem to perfectly align. This synchronism explains the unusual combination of Eosin Y with violet light: the reaction does not proceed *via* the triplet state of Eosin Y, but Eosin Y is rather a precatalyst whose photodissociation forms the actual catalytically active mixture. Interestingly, even though the photolysis of Eosin Y has been previously well characterized together with the establishment of the catalytic activity of the decomposition products of other photocatalysts, to our knowledge, this is the first report detailing the synthetic utilization of Eosin Y degradation products.[19,21] Out of the previously discussed dissociation products, especially the bromine radicals are well known as HAT active species.[21] To test whether the bromine radicals could indeed catalyse our transformation, we set up control experiments using catalytic amounts of tetra-*n*-butylammonium bromide (TBABr) in combination with a photocatalyst capable of oxidizing the bromide anion into a bromine radical.[22] Indeed, the combination of TBABr with an acridinium-derived photocatalyst gave the desired product **2a** in a 36% yield, whereas the acridinium dye alone was not able to catalyse the reaction (Scheme 3c and Table S8). On one hand, this result confirms the feasibility of the bromine radical as the HAT catalyst, but on the other hand, it leaves room for the coexistence of other catalytically active species to reach the efficiency observed under the optimal reaction conditions. Finally, the autocatalytic mechanism was ruled out as the addition of acetophenone to the reaction mixture before irradiation was found to thwart the reaction (see Table S7).

Next, we investigated the processes taking place during the starting material conversion and the product formation phases (stages II + III of the kinetic curve). Although a clear discrepancy

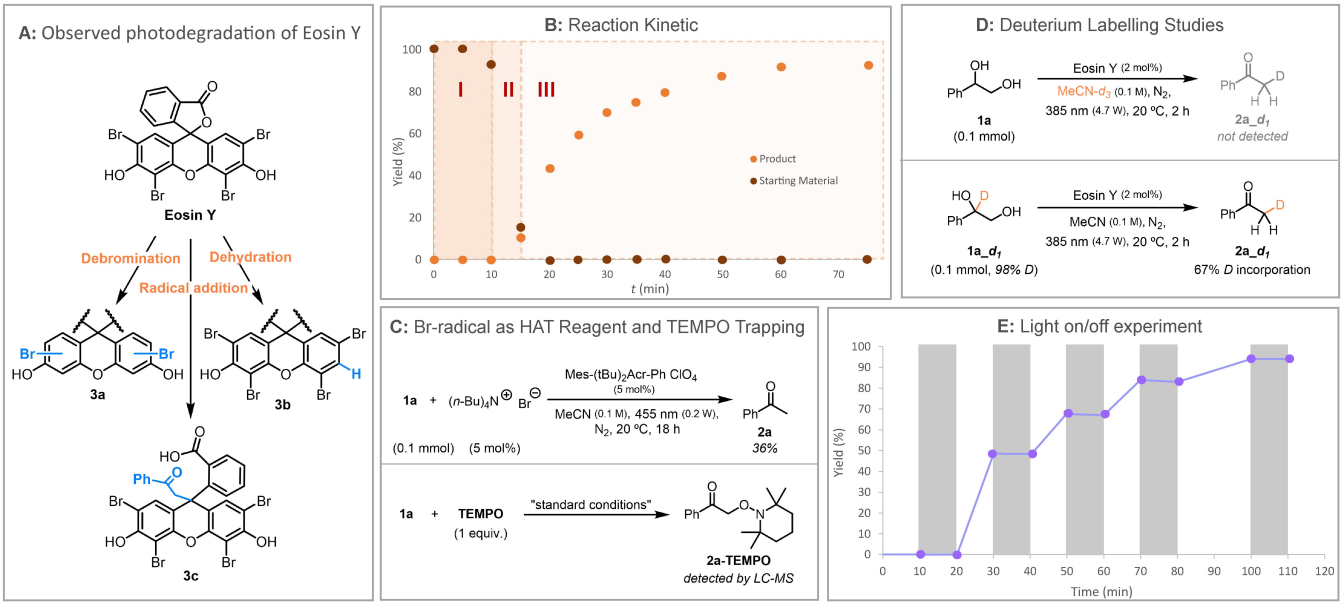

Scheme 3. Observed photodegradation products of Eosin Y in LC–MS analysis (a), kinetic profile of the reaction (b), bromine-radical mediated HAT and TEMPO trapping experiment (c), deuterium labelling experiment (d) and light on/off experiment (e).

could be observed in the rates of these two events, no intermediates could be detected by GC-FID or ^{1}H-NMR analysis of the reaction progress (see SI). However, a radical trapping experiment with TEMPO was able to identify the adduct stemming from the *alpha*-carbonyl radical (**2 a-TEMPO**) supporting the 1,2-spin center shift as a viable reaction pathway (Scheme 3c). Further insights into the behaviour of this radical came from deuterium labelling experiments (Scheme 3d). Running the reaction in deuterated acetonitrile did not result in any deuterium incorporation into the product, which indicates that the solvent does not play any active role in the reaction.[23] Interestingly, a high level of deuterium transfer between the benzylic position and the α-carbonyl position was observed, suggesting that the abstracted hydrogen (or deuterium) atom might end up in the terminal position of the product. This deuteration process could occur either through a back deuterium atom transfer (bDAT) or, through a reductive radical polar crossover, followed by deuteration of the enolate intermediate. Importantly, the former mechanistic pathway, where the *alpha*-carbonyl radical is proposed to abstract a deuterium atom would imminently regenerate the original HAT active species, thus making the process a radical chain reaction. Although the free carbanions have been in turn described as superbasic intermediates able to deprotonate acetonitrile, in our reaction, the possibility for enolate formation would significantly reduce the basicity of these reduced species. Moreover, the performed light on/off experiment verified the necessity of continuous irradiation for the reaction, thus hinting against a radical chain mechanism as the main product-forming pathway (Scheme 3e).

Based on our mechanistic studies and the previous literature on 1,2-spin center shift discussed above, the following reaction mechanism is proposed (Scheme 4). During the induction

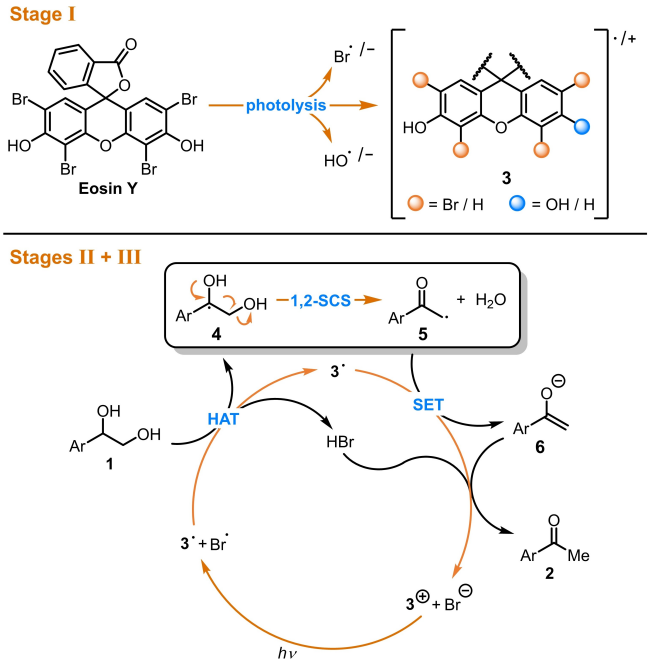

Scheme 4. Proposed reaction mechanism for the photocatalytic redox-neutral dehydration of aryl-1,2-ethanediols.

period of the reaction (stage I), the high energy irradiation forms a highly active catalytic mixture of Eosin Y derivatives **3** and their corresponding elimination products (such as bromine radicals). These HAT active species initiate the product-forming cycle (stages II and III) by abstracting a hydrogen atom from the aryl-1,2-diols **1** forming the benzylic radical **4**. This radical undergoes a rapid 1,2-spin center shift generating an α-carbonyl radical **5** and releasing a molecule of water. The radical intermediate **5** is then reduced to the corresponding enolate **6**,

followed by protonation to product **2**, for example, by the initial hydrogen atom abstracting species. Although the final steps of the mechanism could not be fully ascertained, a photocatalytic regeneration step, such as a SET between $\mathbf{3}^+$ and Br^-, is needed to close the catalytic cycle.

Conclusions

In summary, we have developed a protocol for the photocatalytic dehydration of aryl-1,2-diols to the corresponding methyl ketone derivatives. Our system uses Eosin Y as the sole catalyst and achieves cleavage of water under mild reaction conditions, and without activating reagents or pre-functionalization steps. The mechanistic studies revealed that the reaction is driven by a highly active catalytic mixture formed from the photolysis of Eosin Y. The product-forming cycle features a benzylic hydrogen atom abstraction followed by a 1,2-spin center shift, after which the carbonyl radical is reduced to its enolate form and is finally protonated. Considering the sensitivity of complex (bio)molecules and the conditions typically required in dehydration protocols, we hope that our contribution will inspire further development towards improved methods for elimination reactions.

Experimental Section

General Procedure for the Photocatalytic Dehydration

A 5 mL crimp-cap vial equipped with a Teflon-coated stirring bar, was loaded with the corresponding 1,2-ethanediol (0.1 mmol, 1.0 equiv.) and Eosin Y (1.4 mg, 2.0 μmol, 2 mol%). The vial was sealed, evacuated, and backfilled with N_2 before adding MeCN (1 mL). Then, the resulting mixture was sonicated for 15 s, purged with N_2 for 5 min, and subsequently stirred under irradiation using a 4.7 W 385 nm (±25 nm) LED set-up for 1–18 hours at 20 °C (temperature controlled by a cryostat). After the reaction concluded, four vials were combined, and major impurities were removed by filtering the mixture through a short silica plug using DCM as eluent. The volume of the crude was then carefully reduced to around 10 mL, which was then subjected to flash column chromatography using a mixture of PE/Et_2O as eluent. Careful solvent evaporation yielded the desired products.

General Procedure for Diol Synthesis from Alkenes

The styrene derivative (3.0 mmol, 1.0 equiv.), I_2 (30 mg, 16 μmol, 4 mol%), deionized water (1.5 mL), and *tert*-butylhydroperoxide (70% solution in H_2O, 1.5 mL, 10.8 mmol, 3.6 equiv.) were added to a 15 ml crimp-cap vial. The vial was sealed, and the reaction mixture was heated at 90 °C for 24 h. The reaction was quenched with 2 M $Na_2S_2O_3$ (4 mL) and the product was extracted with EtOAc (5×10 mL). The combined organic layers were dried over $MgSO_4$, the drying agent filtered off, and the solvent removed under reduced pressure. The crude product was purified by flash column chromatography using PE/Acetone as eluent.

General Procedure for Diol Synthesis from Ketones

SeO_2 (1.25 equiv.) was suspended into a mixture of 1,4-dioxane and water (24:1, 1.25 M), and warmed to 55 °C until fully soluble. The mixture was then cooled to room temperature, the acetophenone derivative (5 mmol, 1.0 equiv.) was added and the reaction was heated at reflux (100 °C) overnight. Dark (often green) colored reaction mixture with black precipitate at the bottom was found to be indicative of a successful oxidation. After cooling to ambient temperature, the mixture was filtered and concentrated under reduced pressure. The crude was then pressed through a silica plug using PE/EtOAc (1:1) as eluent and evaporated to dryness.

The crude product was then dissolved in EtOH (0.3 M) and cooled to 0 °C. $NaBH_4$ (2.0 equiv.) was added portionwise, and the reaction was stirred overnight while allowing it to warm to rt. The reaction was quenched with 2 M HCl (or sat. NH_4Cl for acid-sensitive substrates), ethanol was then removed under reduced pressure and, the remaining aqueous mixture was extracted with EtOAc (×3). After drying with $MgSO_4$, the mixture was filtered, and the solvent evaporated. Purification with flash column chromatography (PE/Acetone) yielded the final products.

CAUTION: Due to the toxicity of various selenium compounds, all selenium-containing waste (solids, filterpaper etc.) needs to be disposed carefully.

Supporting Information Summary

The authors have cited additional references within the Supporting Information.[24–31]

Acknowledgements

The project was financially supported by the Deutsche Forschungsgemeinschaft (DFG, German Science Foundation) GRK2620 – 426795949 and TRR325 – 444632635. We kindly thank Dr. Rudolf Vasold, Mr. Ernst Lautenschlanger, and the Department of Mass Spectrometry for their kind assistance. Open Access funding enabled and organized by Projekt DEAL.

Conflict of Interests

The authors declare no conflict of interest.

Data Availability Statement

The data that support the findings of this study are available in the supplementary material of this article.

Keywords: Dehydration · Eosin Y photodegradation · 1,2-spin center shift · Photocatalysis

[1] a) A. C. Weymouth-Wilson, *Nat. Prod. Rep.* **1997**, *14*, 99–110; b) B. La Ferla, C. Airoldi, C. Zona, A. Orsato, C. Cardona, S. Merlo, E. Sironi, G. D'Orazio, F. Nicotra, *Nat. Prod. Rep.* **2011**, *28*, 630–648; c) Y. van Kooyk,

G. A. Rabinovich, *Nat. Immunol.* **2008**, *9*, 593–601; d) A. Helenius, M. Aebi, *Science* **2001**, *291*, 2364–2369.
[2] K. Yamatsugu, M. Kanai, *Chem. Rev.* **2023**, *123*, 6793–6838.
[3] Y. van Kooyk, G. A. Rabinovich, *Nat. Immunol.* **2008**, *9*, 593–601.
[4] a) T. Rice, E. Zannini, E. K. Arendt, A. Coffey, *Crit. Rev. Food Sci. Nutr.* **2019**, *60*, 2034–2051; b) A. R. Pereira, V. C. Fernandez, C. Delerue-Matos, V. de Freitas, N. Mateus, J. Oliveira, *Food Chem.* **2024**, *461*, 140945.
[5] a) Y. Liu, W. Wang, A.-P. Zeng, *Nat. Commun.* **2022**, *13*, 1595; b) H. Tang, Y.-B. Tian, H. Cui, R.-Z. Li, X. Zhang, D. Niu, *Nat. Commun.* **2020**, *11*, 5681; c) C. K. Hill, J. F. Hartwig, *Nat. Chem.* **2017**, *9*, 1213–1221; d) Y. Wang, H. M. Carder, A. E. Wendlant, *Nature* **2020**, *578*, 403–408.
[6] a) K. R. Kunduru, R. Hogerat, K. Ghosal, M. Shaheen-Mualim, S. Farah, *J. Chem. Eng.* **2023**, *459*, 141211; b) A. Delavarde, G. Savin, P. Derkenne, M. Boursier, R. Morales-Cerrada, B. Nottelet, J. Pinaud, S. Caillol, *Prog. Polym. Sci.* **2024**, *151*, 101805; c) A. C. Weymouth-Wilson, *Nat. Prod. Rep.* **1997**, *14*, 99–110.
[7] B. La Ferla, C. Airoldi, C. Zona, A. Orsato, F. Cardona, S. Merlo, E. Sironi, G. D'Orazio, F. Nicotra, *Nat. Prod. Rep.* **2011**, *28*, 630.
[8] a) A. Hu, J.-J. Guo, H. Pan, H. Tang, Z. Gao, Z. Zuo, *J. Am. Chem. Soc.* **2018**, *140*, 1612–1616; b) A. Hu, Y. Chen, J.-J. Guo, N. Yu, Q. An, Z. Zuo, *J. Am. Chem. Soc.* **2018**, *140*, 13580–13585; c) T. Xue, Z. Zhang, R. Zeng, *Org. Lett.* **2021**, *24*, 977–982; d) W. Liu, Q. Wu, M. Wang, Y. Huang, P. Hu, *Org. Lett.* **2021**, *23*, 8413–8418; e) K. Sumiyama, N. Toriumi, N. Iwasawa, *Eur. J. Org. Chem.* **2021**, *2021*, 2474–2478; f) H. G. Yayla, H. Wang, K. T. Tarantino, H. S. Orbe, R. R. Knowles, *J. Am. Chem. Soc.* **2016**, *138*, 10794–10797; g) E. Tsui, A. J. Metrano, Y. Tsuchiya, R. R. Knowles, *Angew. Chem. Int. Ed.* **2020**, *59*, 11845–11849.
[9] J. Schwarz, B. König, *Chem. Commun.* **2019**, *55*, 486–488.
[10] a) D. F. McMillen, D. M. Golden, *Ann. Rev. Phys. Chem.* **1982**, *33*, 493–532; b) M. M. Suryan, S. A. Kafafi, S. E. Stein, *J. Am. Chem. Soc.* **1989**, *111*, 4594–4600.
[11] a) Y.-A. Zhang, X. Gu, A. E. Wendlandt, *J. Am. Chem. Soc.* **2022**, *144*, 599–605; b) C. J. Ostwood, D. W. C. MacMillan, *J. Am. Chem. Soc.* **2022**, *144*, 93–98; c) A. S. K. Lahdenperä, J. Dhankhar, D. J. Davies, N. Y. S. Lam, P. D. Bacoş, K. de la Vega-Hernández, R. J. Phipps, *Science* **2024**, *386*, 42–49.
[12] P. Wessig, O. Muehling, *Eur. J. Org. Chem.* **2007**, *2007*, 2219–2232.
[13] a) F.-L. Zhang, B. Lin, K. N. Houk, Y.-F. Wang, *JACS Au* **2022**, *2*, 1032–1042; b) B. Matsuo, A. Granados, J. Majhi, M. Sharique, G. Levitre, G. A. Molander, *ACS Org. Inorg. Au* **2022**, *2*, 435–454.
[14] a) K. Chen, J. Schwarz, T. A. Karl, A. Chatterjee, B. König, *Chem. Commun.* **2019**, *55*, 13144–13147; b) Q. Zhu, D. G. Nocera, *ACS Catal.* **2021**, *11*, 14181–14187; c) Y.-X. Cao, G. Zhu, Y. Li, N. Le Breton, C. Gourlaouen, S. Choua, J. Boixel, H.-P. Jacquot de Rouville, J.-F. Soulé, *J. Am. Chem. Soc.* **2022**, *144*, 5902–5909.
[15] a) Y. Cheng Kang, S. M. Treacy, T. Rovis, *ACS Catal.* **2021**, *11*, 7442–7449; b) D. Birnthaler, R. Narobe, E. Lopéz-Berguno, C. Haag, B. König, *ACS Catal.* **2023**, *13*, 1125–1132.
[16] a) R. Lechner, S. Kümmel, B. König, *Photochem. Photobiol. Sci.* **2010**, *9*, 1367–1377; b) M. A. Ischay, M. S. Ament, T. P. Yoon, *Chem. Sci.* **2012**, *3*, 2807–2811.
[17] a) X.-Z. Fan, J. W. Rong, H.-L. Wu, Q. Zhou, H.-P. Deng, J. Da Tan, C.-W. Xue, L.-Z. Wu, H.-R. Tao, J. Wu, *Angew. Chem. Int. Ed.* **2018**, *57*, 8514–8518; b) D. M. Yan, Q.-Q. Zhao, L. Rao, J.-R. Chen, W.-J. Xiao, *Chem. Eur. J.* **2018**, *24*, 16895–16901; c) M. Majek, F. Filace, A. J. von Wangelin, *Beilstein J. Org. Chem.* **2014**, *10*, 981–989; d) H. Cao, D. Kong, L.-C. Yang, S. Chanmungkalakul, T. Liu, J. L. Piper, Z. Peng, L. Gao, X. Liu, X. Hong, J. Wu, *Nat. Synth.* **2022**, *1*, 794–803.
[18] Due to the low absorption coefficient of the band around 380 nm, concentration and light path length are important parameters to observe this feature. See detailed measurement conditions in the SI (s42).
[19] A. Alvarez-Martin, S. Trashin, M. Cuykx, A. Covaci, K. De Vael, K. Janssen, *Dyes Pigm.* **2017**, *145*, 376–384.
[20] P. Kimber, F. Plasser, *J. Chem. Theory Comput.* **2023**, *19*, 2340–2352.
[21] a) S. Grotjahn, B. König, *J. Org. Chem.* **2021**, *23*, 3146–3150; b) Y. Kwon, J. Lee, Y. Noh, D. Kim, Y. Lee, C. Yu, J. C. Roldao, J. Gierschner, R. Wannemacher, M. S. Kwon, *Nat. Commun.* **2023**, *14*, 92; c) Y.-X. Cao, G. Zhu, Y. Li, N. Le Breton, C. Gourlaouen, S. Choua, J. Boixel, H.-P. Jacquout de Rouville, J.-F. Soulé, *J. Am. Chem. Soc.* **2022**, *144*, 5902–5909.
[22] a) Z. Wang, X. Ji, T. Han, G.-J. Deng, H. Huang, *Adv. Synth. Catal.* **2019**, *361*, 5643–5647; b) P. Jia, Q. Li, W. C. Poh, H. Jiang, H. Liu, H. Deng, J. Wu, *Chem* **2020**, *6*, 1766–1776.
[23] S. Grotjahn, C. Graf, J. Zelenka, A. Pattanaik, L. Müller, R. J. Kutta, J. Rehbein, J. Roithová, R. M. Gscwind, P. Nuernberger, B. König, *Angew. Chem. Int. Ed.* **2024**, *63*, e202400815.
[24] X. Gao, J. Lin, L. Zhang, X. Lou, G. Guo, N. Peng, H. Xu, Y. Liu, *J. Org. Chem.* **2021**, *86*, 15469–15480.
[25] J. P. G. Rygus, D. G. Hall, *Nat. Commun.* **2022**, *14*, 2653.
[26] B. Zeynizadeh, T. Behvar, *Bull. Chem. Soc. Jpn.* **2005**, *78*, 307–315.
[27] O. Obaro-Best, J. Reed, A. F. B. Norfadilah, R. Monahan, R. Sunasee, *Synth. Commun.* **2016**, *46*, 586–593.
[28] B. D. Dond, S. N. Thore, *Tetrahedron Lett.* **2020**, *61*, 151660.
[29] S.-K. Wang, X. You, D.-Y. Zhao, N.-J. Mou, Q.-L. Luo, *Chem. Eur. J.* **2017**, *23*, 11757–11760.
[30] M. Huix-Rotlant, D. Siri, N. Ferré, *Phys. Chem. Chem. Phys.* **2013**, *15*, 19293–19300.
[31] a) Z. Wang, X. Ji, T. Han, G.-J. Deng, H. Huang, *Adv. Synth. Catal.* **2019**, *361*, 5643–5647; b) P. Jia, Q. Li, W. C. Poh, H. Jiang, H. Liu, H. Deng, J. Wu, *Chem* **2020**, *6*, 1766–1776.

Manuscript received: November 14, 2024
Accepted manuscript online: December 8, 2024
Version of record online: ■■, ■■

RESEARCH ARTICLE

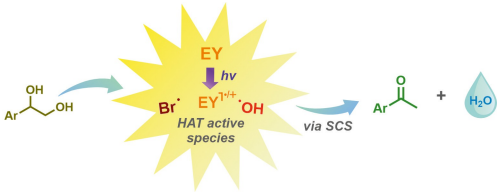

*E. K. Taskinen, D. Kolb, M. Morgenstern, B. König**

"How would you remove water from your molecule with light?" Herein, we report a mild photocatalytic dehydration protocol for aryl-1,2-ethanediols. Our mechanistic studies suggest a hydrogen atom transfer (HAT) and a 1,2-spin center shift (SCS) as key steps. Eosin Y photodissociation products serve as a highly efficient catalytic mixture.